Characterization of a Mn-SOD from the desert beetle *Microdera punctipennis* and its increased resistance to cold stress in *E. coli* cells

5   Zilajiguli Xikeranmu, Ji Ma, Xiaoning Liu*

7   Xinjiang Key Laboratory of Biological Resources and Genetic Engineering, College of Life

8   Science and Technology, Xinjiang University, 666 Shengli Road, Urumqi 830046, China

10   Corresponding Author:
11   Xiaoning Liu
12   Xinjiang Key Laboratory of Biological Resources and Genetic Engineering, College of Life
13   Science and Technology, Xinjiang University, Urumqi 830046, China
14   Email address: liuxn0103@sina.com (Xiaoning. Liu)

Abstract

16   Insects have developed a complex network of enzymatic antioxidant systems for handling
17 reactive oxygen species (ROS) generated during stress. Superoxide dismutases (SODs) play a
18 determinant role in balancing ROS in insect. However, studies devoted to SODs functions in
19 insects under cold stress are limited. In the present study, we attempted to identify and characterize
20 a mitochondrial manganese SOD (mMn-SOD) from the desert beetle *Micordera punctipennis*
21 (denoted as MpmMn-SOD) and explore its protective effects on bacteria cells under cold stress.
22 MpmMn-SOD was composed of 202 amino acids with conserved domains required for metal ions
23 binding and enzyme activity. qRT-PCR experiments revealed that the expression of *MpmMn-SOD*
24 was ubiquitous but tissue-specific and was induced by cold stress. An *E. coli* system (BL21) was
25 applied to study the function of MpmMn-SOD. The MpmMn-SOD gene was cloned into the
26 prokaryotic expression vector pET-32a to generate a recombinant plasmid pET-32a(*MpmMn-*
27 *SOD*). After transformation of the plasmid into *E. coli* BL21, the fusion proteins Trx-His-MpmMn-
28 SOD was overexpressed and identified by SDS-PAGE and Western blotting. The transformed
29 bacteria BL21 (pET32a-mMn-SOD) showed enhanced cold resistance compared to the control
30 bacteria BL21 (pET32a). Its SOD activity under -4 ℃ had a significant negative correlation ($r =$-
31 0.995) with superoxide anion $O_2 \bullet^-$ contents. Antioxidant activity assay showed that the death zones
32 of BL21 (pET32a-mMn-SOD) were smaller in diameter than the control bacteria. Accordingly,

33   the transformed bacteria had lower electric conductivity and malondialdehyde (MDA) contents

34   than the control bacteria under cold stress. Taken together, our results showed that cold stress

35   stimulated the expression of *MpmMn-SOD* in *M. punctipennis*. The *E. coli* cells that overexpress

36   MpmMn-SOD could increase their resistance to cold stress by scavenging ROS, and mitigate

37   potential cell damage caused by ROS under cold conditions.

38   **Introduction**

39   Oxygen is essential for most life forms. The full reduction of oxygen to H_2O by cytochrome

40   oxidase is a key step in the mechanism of aerobic ATP formation (*Hermes-Lima et al., 2001*).

41   However, the partial reduction of oxygen leads to the formation of various reactive oxygen species

42   (ROS). Superoxide anion radical ($O_2\bullet^-$) is usually the first ROS to be generated. The equilibrium

43   between the production and the scavenging of ROS may be perturbed by various biotic and abiotic

44   stress factors such as salinity, UV radiation, drought, heavy metals and temperature extremes

45   (*Sarvajeet Singh & Narendra, 2010*). Insects are constantly subjected to changes in environmental

46   temperature. Low temperature is a major environmental constraint that impacts the geographic

47   distribution and seasonal activity patterns of insects (*Denlinger DL, 2010*). Cold stress may result

48   in oxidative stress with the accumulation of ROS (*Gharari et al., 2014; Jithesh et al., 2006*).

49   Unbalanced high levels of ROS in living organisms under stress can cause potential damage

50   to biological macromolecules (*Jaramillo-Gutierrez et al., 2010*). To defend against the oxidative

51   injury of ROS, cells are equipped with myriad antioxidant enzymes to scavenge and detoxify the

52   accumulated oxyradicals (*Arenas-Ríos et al., 2007; Park SY, 2004; Vaughan, 1997*). Enhanced

53   antioxidants could provide this same action to support winter survival by cold-hardy insects

54   (*Denlinger DL, 2010*). The dominant ROS, superoxide anion ($O_2\bullet^-$), is converted to hydrogen

55   peroxide (H_2O_2) by superoxide dismutase (SOD), then transformed to water via catalase (CAT) or

56   glutathione peroxidase (GPx) (*Felton and Summers, 1995; Schafer and Buettner, 2001*).

57   SODs are the main antioxidant enzyme families in organisms, they are considered as the first

58   defense line against oxidative stresses by converting $O_2\bullet^-$ to H_2O_2 and H_2O (*Ackerman & Brinkley,*

59   *1966; McCord & Fridovich, 1988*). SOD is unique in that its activity determines the concentration

60   of O_2 and H_2O_2, the two Haber-Weiss reaction substrates, and it is therefore central in the defense

61   mechanism (*Bowler, 1992*). SODs are classified into three distinct groups in eukaryotes:

62   intracellular copper/zinc SOD (icCuZn-SOD), extracellular copper/zinc SOD (ecCuZn-SOD, or

63   EC-SOD) and manganese SOD (Mn-SOD) (*Zelko et al., 2002*).

64   Mn-SOD has received much attention because mitochondria is the main source of ROS

65   (*Kailasam et al., 2011; Li et al., 2011*). Two types of Mn-SOD are known in eukaryotes:

66   mitochondrial Mn-SOD (mMn-SOD) that has a mitochondrial transit peptide for translocation and

67   cytosolic Mn-SOD (cMn-SOD) without the peptide (*Lin et al., 2010*). Temperature stress was

68   reported as one of the key mediators of ROS generation (*Harari et al., 1989; Rauen et al., 1999*).

69   The mitochondrial electron-transport chain is responsible for a significant proportion of

70   intracellular superoxide radical production (*Møller, 2010*). Low temperature can fall down the rate

71   of enzymatic reactions, leading to a decrease in demand for ATP and accumulation of electrons in

72   certain points of the respiratory chain. This situation promotes a sudden increase in the production

73   of several ROS which relieve the burden of excess reducing potential. Cold stress is therefore

74   associated with an increased intracellular oxidative stress, and an increase in antioxidants activity

75   appears to be one of features of cold-adaptations (*Chattopadhyay, 2002*). Previous studies have

76   shown that the expression of *Mn-SOD* gene is induced in response to cold stress in several insect

77   species (*Kim et al., 2010; Gao XL et al., 2013; Gao XM et al., 2013; Jia et al., 2014*). Beetle

78   *Micordera punctipennis* (Coleoptera: Tenebrionidae) is an endemic species in Gurbantunggut

79   Desert in Xinjiang, China (*Hou et al., 2010*). The adult is cold hardy, the average temperatures of

80   the soil surface and soil-in-5cm in January were -12 ℃ and -5 ℃, respectively (*Huang et al., 2005*).

81   In the low temperature transcriptome of *M. punctipennis*, GO (Gene ontology) term analysis

82   showed that Mn-SOD is one of the eight significantly up-regulated genes that are related to abiotic

83   stress response (*Tusong et al., 2016*). It is possible that Mn-SOD might be present in the

84   mitochondrial matrix, near the primary source of superoxide, as occurs in other species and may

85   respond to oxidative stress caused by cold stress. However, the function and characteristics of this

86   protein in *M. punctipennis* are currently unclear. In this study we aim at (1) isolating and

87   characterizing a mitochondrial Mn-SOD gene (*MpmMn-SOD*) from *M. punctipennis*; (2)

88   investigate *MpmMn-SOD* distribution patterns in different tissues and temporal expression profiles

89   at mRNA level after being challenged by low temperature in order to explore one of the possible

90   mechanisms of the insect response to cold stress; (3) analyzing the antioxidant activity of the

91   recombinant MpmMn-SOD and the $O_2\bullet^-$ contents under cold stress by over-expressing this protein

92   in bacteria.; (4) examining the protective effects of MpmMn-SOD on the bacteria cells carrying

93   *MpmMn-SOD* gene under cold stress. The results will help to primarily study the possible function

94   of MpmMn-SOD in the desert beetle under cold conditions.

95   **Materials & Methods**

96   **Insect treatments, total RNA extraction and cDNA synthesis**

97   The beetles were collected from Wujiaqv (N 44° 29′, E 87° 31′, 410 m), which is about 100

98   km northeast of the geological center of Asia. The samples were returned to the laboratory and

99   kept in large plastic beakers containing dry sands at 30 ± 0.5 ℃, 16:8 h (light: dark) photoperiod,

100   relative humidity (RH) of 30 ± 6%. Adults were fed with wheat bran and fresh cabbage leaves.

101   Beetles were dissected in cold 1×PBS (phosphate belanced solution) to isolate different

102   tissues, such as head, midgut, hindgut (containing Malpighian tubule), fat body and carcass (whole

103   body after head, gut and fat body were removed).

104   As 4℃ is the low temperature at which the insect has begun to respond to cold stress (*Hou et*

105   *al., 2010*), the beetle individuals were exposed at 4 ℃ for different time periods (0.5 h, 1 h, 1.5 h,

106   2 h, 3 h, 5 h, 7 h, 9 h and 11 h, respectively, three replicates per treatment group). The individuals

107   at room temperature (about 25 ℃) without any cold treatment were used as control. After the cold

108   treatment, beetles were immediately frozen in liquid nitrogen for RNA extraction. Total RNA

109   extraction was performed by using Trizol reagent (Invitrogen, Carlsbad, CA) following the

110   manufacturer's protocol. RNA concentration was quantified by using a Nano-Drop ND-1000

111   spectrophotometer (NanoDrop Technologies, Wilmington, USA). The cDNA was synthesized

112   from 1.0 µg total RNA based on Reverse Transcriptase M-MLV (Takara, China) according to the

113   manufacturer's instructions.

114   **Cloning of the full-length *MpmMn-SOD* cDNA**

115   *MpmMn-SOD* fragment (transcriptomic ID c41919) which had the up-regulated expression

116   at 4 ℃ was selected from the transcriptomic data of *M. punctipennis* (*Tusong et al., 2017*). The

117   lacked 3'-sequence were obtained by SMARTer™ RACE cDNA Amplification Kit (Clontech,

118   Beijing, China). Primers used in this experiment were detailed in Table 1. The PCR program was

119   95 ℃ for 5 min followed by 30 cycles of 94 ℃ for 30 s, 63 ℃ for 30 s, 72 ℃ for 1 min and a final

120   extension at 72 ℃ for 10 min. For verification, PCR products were purified, and cloned into

121   pMD18-T vector (Trans GenBiotech, Beijing, China), and then were transformed into competent

122   *E. coli* cells (DH5a) for Sanger sequencing by Quintarabio, Urumqi, China.

123   The deduced amino acid domains in MpmMn-SOD were analyzed using the BLAST search

124   program (http://blast.ncbi.nlm.nih.gov/ Blast.cgi). The physicochemical properties were predicted

125   by using AntPASy's ProtParam Online Tool. Multiple sequence alignments among insect species

126   in different orders were created with DNAMAN 6.0 software (http://www.lynnon.com). The signal

127   peptide cleavage site was examined with SignalP 4.1 (http://www.cbs.dtu.dk/services/SignalP/)

128   program. TargetP 1.1 (http://www.cbs.dtu.dk/ services/TargetP/) was used to predict presence of

129 a putative mitochondrial targeting sequence (MTS). Phylogenetic analysis was performed by

130 IQTREE 1.6.2. The phylogenetic tree was constructed based on predicted amino acid sequences

131 using the Maximum Likelihood (ML) method with 5000 replicates bootstrap. Mn-SOD sequences

132 in different insect species were downloaded from the database in NCBI website.

133 **mRNA level of *MpmMn-SOD* detected by Fluorescent real-time quantitative PCR (RT-**

134 **qPCR)**

135 The expression of *MpmMn-SOD* transcript was assayed on a 7500 Real Time PCR System

136 (Applied Biosystems, USA) using SYBR Green Mix to determine the expression profiles of

137 *MpmMn-SOD* gene in *M. punctipennis* at 4 ℃ for 0.5~11 h as described above. Translation

138 elongation factor (*EF-α*) was used as a reference gene to normalize the target gene expression

139 levels among samples (*Xikeranmu et al., 2019*). Primers for RT-qPCR are detailed in Table 1

140 . The qPCR amplification conditions were 94 ℃ for 2 min, followed by 40 cycles at 94 ℃ for

141 30 s and 62 ℃ for 30 s. The relative expression of the target gene was calculated using the

142 comparative $2^{-\Delta\Delta CT}$ method. The change of the gene expression levels at 4 ℃ was normalized to

143 the gene in the control at 25 ℃.

144 The expression of *MpmMn-SOD* mRNA in head, midgut, hindgut, fat body and carcass were

145 separately detected by RT-qPCR. The expression level of *MpmMn-SOD* in different tissues was

146 normalized to that of the head which had the lowest expression level. The value at each time point

147 was given as mean ± *S.E.* (*n*=3).

148 **Prokaryotic expression and Western blot analysis of the fusion protein Trx-His- MpmMn-**

149 **SOD**

150 To obtain the recombinant MpmMn-SOD protein and examine whether it possesses

151 antioxidant activity, DNAMAN was used to design primers containing *Bam*HI and *Xho*I restriction

152 sites (Table 1) to amplify the coding sequence (CDS) of *MpmMn-SOD* gene. The amplified

153 fragments were digested with the endonucleases, and subcloned into a pET-32a (+) expression

154 vector that was digested with the same enzymes. The constructed plasmid denoted as pET-32a

155 (MpmMn-SOD) was transformed into competent cells of *E. coli* BL21 (DE3). The parent vector

156 pET-32a without inserts gene was transformed into BL21 (DE3), and used as a control. The two

157 transformed bacteria were induced with 0.5 mM isopropyl β-D-thiogalactoside (IPTG) at 25 ℃ for

158 10 h to overexpress fusion proteins Trx-His-MpmMn-SOD (41 kDa) and Trx-His (the tag protein

159 on the vector, 18.5 kDa) respectively in *E. coli*. Luria broth (LB) was used for bacterial culture

160 medium. Expression efficiency of different transformants was assessed by analysis of the target

Table 1

161 protein band in dodecyl sulfate, sodium salt (SDS)-Polyacrylamide gel electrophoresis (SDS-

162 PAGE). The correct expression of the proteins was further confirmed by Western blotting with

163 anti-His antibody (Zsbiotech, Beijing, China).

164

165 **Measurement of SOD activity and $O_2\bullet^-$ content in the MpmMn-SOD overexpressed bacteria**

166 **at -4 ℃**

167 As 4 ℃ is not enough to influence bacteria survival within short time, we treated the

168 MpmMn-SOD overexpressed bacteria under -4 ℃. BL21(pET-32a) were set as the control.

169 Cultures of the two bacteria were induced to produce proteins Trx-His-MpmMn-SOD and Trx-His

170 separately by addition of IPTG described above, and 5 mL cultures of the bacteria were exposed

171 to -4 ℃ for 0 h, 2 h, 4 h and 6 h, respectively. At the end of the cold treatments, the bacteria in

172 each group were recovered at 37 ℃ for 1 h, and OD595 was determined for making survival curve.

173 The control was -4 ℃ for 0 h no cold treatment. Each treatment had three replicates.

174 Then, the cells were harvested by centrifugation (12000 rmp,10 minutes, at 4 ℃). The

175 collected cells were sonicated in an ice bath after suspension in PBS. The supernatants were

176 collected as crude enzyme liquids and were quantified using the BCA Protein Assay Kit (Thermo

177 Scientific Pierce, IL, USA). $O_2\bullet^-$ content was measured according to the hydroxylamine oxidation

178 method described by Wang et al (*Wang & Luo, 1990*). The SOD activity was detected using the

179 CuZn/Mn-SOD Assay Kit (Jiancheng, Nanjing, China) following the manufacturer's protocol with

180 minor modification (*Meng et al., 2013*).

181 The increase of SOD activity was calculated by subtracting the SOD activity of BL21(pET-

182 32a-MpmMn-SOD) from that of the control BL21(pET-32a), then dividing the difference by the

183 SOD activity of BL21(pET-32a-MpmMn-SOD). So, did for calculating the decrease of $O_2\bullet^-$

184 content.

185 **Antioxidant activity assay by the Oxford Cup method**

186 To test whether MpmMn-SOD has antioxidant activity, the tolerance to hydroperoxide of the

187 *E. coli* cells overexpressing Trx-His-MpmMn-SOD was determined by the Oxford Cup method

188 (*Liu, 2018*). The bacteria BL21(pET-32a-MpmMn-SOD) and BL21(pET-32a) were grown

189 overnight at 37 ℃ in LB (Luria-Bertani) broth containing ampicillin (Amp$^+$) (50 mg/L), and then

190 diluted 1: 100 in LB medium. The diluted cells were further incubated at 37 ℃ until a final optical

191 density of 0.4~0.6 at 595 nm. These cells were induced with 0.3 mM IPTG at 25℃ for 10 h. Then,

192 100 μL BL21(pET-32a-MpmMn-SOD) and BL21(pET-32a) were, respectively, added to fresh LB

193   (Amp$^+$) solid medium in plates. After the medium is solidified, five Oxford cups were placed on

194   the plate, then 100 μL of different concentrations (100, 75, 50, 25 and 0 mmol/L) of H$_2$O$_2$ were

195   added to the top of the oxford cup. The plate was incubated overnight at 37 ℃. Three replicates

196   per treatment group. BL21(pET-32a) cells were used as the control. The agent diffused into the

197   surrounding area through the Oxford Cup to form a decreasing concentration gradient. Observe

198   the zone of inhibition formed around the cup and record the diameter of the zone. The inhibition

199   zones were measured as described by Burmeister et al. (*Burmeister et al., 2008*).

200   **Measurement of the Relative electrical conductivity (REC) and Malondialdehyde (MDA)**

201   **content of bacteria BL21(pET-32a-MpmMn-SOD) under -4 ℃**

202   The influence of low temperature on cell membrane permeability was determined by

203   measuring the relative electrical conductivity (REC) in bacteria BL21(pET-32a-MpmMn-SOD)

204   and BL21(pET-32a), respectively. BL21(pET-32a) was used as the control. After the recombinant

205   protein was expressed by IPTG induction, 5 mL of the bacteria were centrifuged at 6000 rpm for

206   10 min to collect cells. The cells were washed with 5% dextrose solution until the bacterial

207   solution's REC (denoted as L1) was comparable to that of 5% glucose solution. Set 5 mL of the

208   isotonic bacterial solutions at −4 ℃ for 0 h, 2 h, 4 h and 6 h, respectively, then measure the REC

209   (denoted as L2) respectively. After boiling for 5 min, the REC (denoted as L0) of the treated

210   bacteria solution was measured again. The final relative conductivity is calculated as: REC (%)

211   =100× (L2 -L1)/L0.

212   For MDA determination, after IPTG induction 5 mL of the cultures were exposed at −4 ℃

213   for 0 h, 2 h, 4 h and 6 h, respectively. Then, 400 μL MDA extract solution (MDA Assay Kit,

214   Solarbio, Beijing, China) were added to the bacteria cells (about two million) to lyse the cells. The

215   mixture was centrifuged at 8000 rpm for 10 min at 4 ℃. The supernatant was collected and set on

216   ice bath. The MDA content was determined by using MDA Assay Kit (Solarbio, Beijing, China)

217   according to the manufacturer's protocol.

218   **Statistical analysis**

219   One-way analysis of variance and Tukey's multiple comparison test were conducted for data

220   analysis in gene expression, SOD activity as well as O$_2$•$^-$ content. Paired *t*-test was employed for

221   data analysis in diameter of inhibition zone, relative conductivity and MDA content. Spearman's

222   correlation analysis was used for correlation analysis of SOD activity and O$_2$• content. Data were

223   shown as mean ± *S.E*.

224 **Commonly used acronyms**

225 thioredoxin–histone(Trx-His), intracellular copper/zinc superoxide dismutase(icCu-Zn/SOD),

226 extracellular copper/zinc superoxide dismutase(ecCuZn-SOD or EC-SOD), cytosolic manganese

227 superoxide dismutase(cMn-SOD),isopropyl β-D-thiogalactoside (IPTG), mitochondrial targeting

228 sequence (MTS), Gene ontology(GO), relative humidity(RH), phosphate belanced solution(PBS),

229 dodecyl sulfate, sodium salt (SDS)-Polyacrylamide gel electrophoresis(SDS-PAGE), Luria-

230 Bertani(LB), Relative electrical conductivity(REC).

231

Results

233 **Identification and characterization of the MpmMn-SOD sequence**

234   We obtained the *MpmMn-SOD* sequence from the transcriptomic data of *M. punctipennis*,

235 and then confirmed this sequence by cDNA cloning. The full-length cDNA was 1359 bp including

236 an ORF of 609 bp, a 3'-UTR of 750 bp with a poly (A) tail and a single polyadenylation signal

237 (AATAAA). The open reading frame (ORF) was 609 bp encoding a protein of 202 amino acids

238 (GenBank accession no. MK676072.1), no signal peptide was predicted. It was predicted as a Mn-

239 SOD sequence containing one N-glycosylation site (NGTL) (circled in Fig.1). The calculated

240 molecular mass was 22 kDa, and the estimated pI was 6.54. Analyses using the online tool TargetP

241 revealed a putative N-terminal mitochondrial targeting sequence (MTS) consisting of 12 amino

242 acids (underlined in Fig.1), indicating this protein may exist in mitochondria. We designated this

243 sequence MpmMn-SOD.

Fig 1

244

245 **Fig 1. Nucleotide and deduced amino acid sequences of a Mn-SOD from the beetle *M.**
246 ***punctipennis*.** The letters in box indicate the start codon (ATG) and the stop codon (TAA). The
247 putative mitochondrial targeting sequence (MTS) is underlined in black. The putative
248 polyadenylation signal (AATAAA) and poly A are underlined in blue. The potential N-
249 glycosylation site is shown in pink (NGTL). The Mn-SOD signature motif (DIWEHAYY) is
250 highlighted in cyan. The four highly conserved amino acids (His26, His76, Asp162, and His166)
251 critical for Mn-binding are circled in red.

252   Comparison of the predicted amino acids of MpmMn-SOD with Mn-SODs from different

253 insect species indicated the high conservation of four manganese binding sites (His26, His76,

254 Asp162 and His166), and one signature of Mn-SOD from 162 to 169 (DV/IWEHAYY) was also

255   conserved across these insect species (Fig. 2). MpmMn-SOD was most like the yellow meal worm

256   Mn-SOD, the two sequences both had a shortened N-terminal sequence compared to Mn-SODs

257   from insects in other taxonomic order. However, the identity of these two sequences was only

258   35.27%, suggesting that MpmMn-SOD was a novel Mn-SOD in insects.

259

260

Fig 2

261   **Fig 2. Multiple alignments of the deduced amino acid sequences of the Mn-SODs from the**
262   **beetle *M. punctipennis* and other known insect species.** The Mn-SOD signature DIWEHAYY
263   is boxed in red (labeled Signature). Mn-binding sites are indicated with triangles. The amino acid
264   homology up to 100% is shown in black, 75% ~99% is in pink and 50% ~74% in cyan. *M.*
265   *punctipennis*: *Microdera punctipennis; T. molitor: Tenebrio molitor; A. mellifera*: *Apis mellifera;*
266   *B.tabaci: Bemisia tabaci; H.armigera: Helicoverpa armigera; T. castaneum: Tribolium*
267   *castaneum.*

268   To further analyze MpmMn-SOD sequence with SOD sequences in other insects at

269   evolutionary perspective, phylogenetic analysis was conducted. The results revealed two separate

270   clusters, Mn-SOD and Cu/Zn-SOD, in the phylogenetic tree with strong bootstrap (100%) support,

271   in accordance with their distinct metal cofactor requirements (Fig. 3). MpmMn-SOD was clustered

272   with Mn-SODs. Within Cu/Zn-SOD clade, ecCu/Zn-SOD and icCu/Zn-SOD were classified as

273   two subgroups with strong bootstrap support (98%), and ecCu/Zn-SOD subgroup was the basic

274   form. MpmMnSOD was closed to the Mn-SOD from the yellow meal worm *Tenebrio molitor*.

Fig 3

275   **Fig 3. Phylogenetic analysis of SOD sequences from *M. punctipennis* and other insect species**
276   **based on predicted amino acid sequences.** *A.cerana cerana: Apis cerana cerana; A. glabripennis:*
277   *Anoplophora glabripennis; A. planipennis: Agrilus planipennis; A.rosae: Athalia rosae; A.*
278   *tumida: Aethina tumida; B.mori: Bombyx mori; B.tabaci: Bemisia tabaci; C.formosanus:*
279   *Coptotermes formosanus; C. lapponica: Chrysomela lapponica. D. helophoroides: Dastarcus*
280   *helophoroides; D.melanogaster: Drosophila melanogaster; D.plexippus: Danaus plexippus;*
281   *G.morsitans morsitans: Glossina morsitans morsitans; H.saltator: Harpegnathos saltator; M.*
282   *punctipennis: Microdera punctipennis; O.biroi: Ooceraea biroi; P. coochleariae: Phaedon*
283   *cochleariae;   T. castaneum: Tribolium castaneum; T. molitor: Tenebrio molitor; Z. nevadensis:*
284   *Zootermopsis nevadensis.*

285   **Expression of *MpmMn-SOD* gene in different tissues**

286   To examine the tissue distribution profile of *MpmMn-SOD* expression, the mRNA levels from

287   head, midgut, hindgut, fat body and carcass were measured by using RT-qPCR. The results showed

288 that *MpmMn-SOD* expressed in all the tissues we have checked, but the expression levels varied

289 greatly among the tissues. The highest was in hindgut followed by fat body, midgut and carcass;

290 the lowest was in head (Fig. 4A). Compared to that of the head, the expression level in hindgut,

291 fat body, midgut and carcass was 57-fold, 17-fold, 5.3-fold and 3.5-fold of that of the head,

292 respectively ($F_{(4,10)} = 111.645$, $P < 0.01$), suggesting a tissue specific expression pattern.

293

Fig 4

Fig 4. Relative mRNA levels of *MpmMn-SOD* gene detected by RT-qPCR. (A) The expression profile of *MpmMn-SOD* gene in different tissues. Values are represented as fold change compared to that of the head; **(B)** Temporal expression of *MpmMn-SOD* gene under 4 ℃ cold stress. Values are represented as fold change compared to the control (0 h). Different letters above each column indicate statistical significance. *P*<0.05 (lower-case letters), *P*<0.01(capital letters).

Temporal expression of *MpmMn-SOD* in *M. punctpennis* at 4 ℃

To determine the effect of cold stress on the expression of *MpmMn-SOD*, the beetles were exposed to 4 ℃ for different time periods, as 4 ℃ is the low temperature at which the insect has begun to respond to cold stress. The results showed that the mRNA level of *MpmMn-SOD* was significantly increased after the cold exposure compared with the control (25 ℃), and this simulative effect was very significant ($F_{(9,18)}$ = 80.07, $P < 0.001$) (Fig. 4B). It was approximately 9.9-fold, 22.5-fold and 125-fold of the control after cold exposure for 0.5 h,1 h and 1.5 h ($P < 0.01$) respectively. The second large expression peak appeared at 11 h, which was about 67.3-fold of the control. From 2 h to 9 h the level slightly fluctuated with a small peak of 16-fold of the control at 3 h. This cold expression profile presented a stress-responsive pattern. The large fluctuation of *MpmMn-SOD* expression during the cold treatment indicated that cells could adjust the level of the enzyme timely and finely.

Prokaryotic expression and Western blot analysis of the fusion protein Trx-His- MpmMn-SOD

To study the enzyme activity of MpmMn-SOD, we inserted MpmMn-SOD into pET32a expression vector and transformed *E. coli* BL21 with this recombinant plasmid. pET32a alone was also transformed into *E. coli* BL21 as the control. The fusion protein Trx-His-MpmMn-SOD and the tag protein Trx-His were separately over-expressed in the two transformants through IPTG induction. The expression of these two proteins were analyzed on SDS-PAGE (Fig. 5A). A clear thick band of about 41 kDa appeared in lane 4 after IPTG induction, it matched the calculated size of the molecular mass of Trx-His-MpmMn-SOD; and a clear thick band of about 18.5 kDa appeared in lane 2 after IPTG induction, it matched the calculated size of the molecular mass of Trx-His. The two proteins were absent in the un-induced samples. We further confirmed the fusion protein by Western blotting using anti-His antibody (Fig. 5B). The result indicated that the fusion protein Trx-His-MpmMn-SOD was correctly expressed in *E. coli*.

Fig 5

325 **Fig 5. Analysis of the fusion protein Trx-His-mMpMn-SOD overexpressed in BL21 cells. (A)**
326 SDS-PAGE analysis of the whole cell lysate. **(B)** Western blot analysis. M: protein marker; lane1:
327 non-induced BL21(pET32a); lane2: induced BL21(pET32a); lane3: un-induced BL21(pET32a-
328 mMn-SOD); lane4: induced BL21 (pET32a-mMn-SOD).

329 **The tolerance of the MpmMn-SOD overexpressed BL21 (pET32a-mMn-SOD) to oxidative**

330 **stress**

331   Antioxidant activity assay was performed to evaluate whether the overexpress mMpMn-SOD
332 could enhance the tolerance of BL21 (pET32a-mMn-SOD) to oxidative stress. The results showed
333 that the death zones around the discs on the BL21 (pET32a-mMn-SOD) plate were smaller in
334 diameter than the control BL21 (pET32a) (Fig. 6A). The diameters of the inhibit zones on agar
335 plates were significantly smaller than the control bacteria (Fig.6B), demonstrating that the mMn-
336 SOD-overexpressing *E. coli* was more tolerant to H_2O_2-mediated oxidative damage than the
337 control BL21 (pET32a).

Fig 6

338
339 **Fig 6. Antioxidant activity assay on LB agar plates containing *E. coli* cells overexpressing**
340 **MpmMn-SOD. Oxford cups containing different concentrations of H_2O_2 were used to**
341 **generate oxidative stress to the cells. (A)** Inhibited zones of the bacteria on agar plates. Numbers
342 1~4 on each disc represents different H_2O_2 concentrations from 100 mM to 25 mM. mMn-SOD:
343 *E. coli* cells BL21(pET32a-mMn-SOD); Control: *E. coli* cells BL21(pET32a). **(B)** Quantitative
344 diameters of the inhibited zones in histograms. Values are compared to the control bacteria
345 between the same group. The data are the mean ± *S.E.* of three replicate

346 **Survival of the MpmMn-SOD overexpressed BL21(pET32a-mMn-SOD) under cold stress at**

347 **-4 ℃**

348   As *E. coli* is not significantly harmed by exposure to 4 ℃ for a limited time, we exposed the
349 MpmMn-SOD overexpressed bacteria BL21(pET32a-mMn-SOD) to −4 ℃ to test the protective
350 function of MpmMn-SOD for the bacteria under cold stress. The survival curve of BL21(pET32a-
351 mMn-SOD) was a convex type, while it was a rough negative line for the control bacteria (Fig.7),
352 indicating the cold resistance of BL21(pET32a-mMn-SOD) was significantly increased compared
353 to the control bacteria BL21(pET32a). The OD595 of BL21(pET32a-mMn-SOD) was 0.63 at 4 h
354 of the cold treatment, which was significantly higher than the control bacteria of 0.52 under the
355 same conditions.

356

Fig 7

357 **Fig.7. Survival curve of the MpmMn-SOD overexpressed BL21 (pET32a-mMn-SOD) at -4**

358 **℃**

359   We detected the changes of the SOD activity and $O_2\bullet^-$ content in the MpmMn-SOD

360 overexpressed bacteria after -4 ℃ treatment. The results showed that the cold stress significantly

361 stimulated SOD activity of BL21(pET32a-Mn-SOD) compared to BL21(pET32a) (Fig. 8A),

362 suggesting the over-expressed MpmMn-SOD in bacteria not only increased SOD activity overall,

363 but also enhanced the response of SOD activity of the cells to cold stress. Accordingly, the $O_2\bullet^-$

364 content in BL21(pET32a-Mn-SOD) was significantly lower than the control bacteria, suggesting

365 that the over-expressed MpmMn-SOD effectively scavenged $O_2\bullet^-$ in cells (Fig. 8B). Pearson's

366 correlation analysis showed that the SOD activity and $O_2\bullet^-$ content of BL21(pET32a-Mn-SOD)

367 under -4 ℃treatment were strong negatively correlated, and the correlation coefficient was -0.995

368 ($p<0.05$). The relative increase of SOD activity at 2 h and 6 h of the cold treatment was 2.3 and 2

369 times of those of the control (Fig.8C). Correspondingly, at 2 h and 6 h time points the relative

370 decrease of $O_2\bullet^-$ content (Fig.8D) was high. The two indexes had similar changing trends,

371 suggesting that the more increase in SOD activity, the more decrease in $O_2\bullet^-$ content under -4 ℃

372 temperature.

373

Fig 8

374 **Fig. 8. SOD activity and $O_2\bullet^-$ content in bacteria BL21 in response to -4 °C cold stress. (A)**
375 SOD activity in bacteria BL21 (pET32a) and (pET32a-mMn-SOD). **(B)** $O_2\bullet^-$ content in bacteria
376 BL21 (pET32a) and (pET32a-mMn-SOD).   **(C)** Relative increase in SOD activity. **(D)** Relative
377 decrease in $O_2\bullet^-$ content. Different letters over each column indicate statistical significance, $P <$
378 0.05.

379 **Relative electrical conductivity (REC) and Malondialdehyde (MDA) content of the MpmMn-**

380 **SOD overexpressed BL21 (pET32a-mMn-SOD) under cold stress at -4 ℃**

381   The excessive accumulation of ROS under cold stress may cause lipid peroxidation which

382 leads to damage of cell membranes. Therefore, electrolyte leakage and MDA level in the BL21

383 (pET32a-mMn-SOD) and the control BL21 (pET32a) under -4 ℃ cold stress were determined.

384 After cold stress, the two groups of bacteria showed increased REC and MDA content (Fig.9),

385 indicating that -4 ℃ caused cells damage to both groups. However, the increasing trends of the

386 two indexes in BL21(pET32a-mMn-SOD) were slower than those of the control BL21(pET32a)

387 during the cold treatment. At 4 h and 6 h of the cold treatment, both REC and MDA content in the

388   control group were significantly higher than the experimental group (Fig. 9A, 9B), indicating that

389   the cell membrane injury in BL21(pET32a-mMn-SOD) caused by the cold stress was less serious

390   than that in the control bacteria. These results suggested that the overexpressed MpmMn-SOD

391   conferred cold tolerance to cells via increasing their ability for ROS-scavenging thus reducing

392   membrane damage.

393

Fig 9

394   **Fig 9. Protective effect of MpmMn-SOD on bacteria BL21(pET32a-mMn-SOD) in response**

395   **to -4 °C cold stress. (A)** Relative conductivity of BL21(pET32a-mMn-SOD) and BL21(pET32a)

396   under -4 °C. **(B)** MDA content of BL21 (pET32a-mMn-SOD) and BL21 (pET32a) under -4 °C.

397   Paired t-test was conducted to analyze the difference between BL21 (pET32a-mMn-SOD) and

398   BL21 (pET32a) at each time treatment group. The symbol * indicates statistical significance $P <$

399   0.05. Values are expressed as means $\pm S.E.$ (n=3).

400

Discussion

402   When insects suffer from environmental stresses such as extreme temperatures, reactive

403   oxygen species (ROS) are spawned (*Gao XM et al., 2013*). Metalloenzyme SOD is the most

404   effective intracellular enzymatic antioxidant which is ubiquitous in all aerobic organisms and in

405   all subcellular compartments prone to ROS mediated oxidative stress. It removes highly toxic $O_2 \bullet^-$

406   and hence prevents the risk of hydroxyl radical OH• generation via the metal catalyzed Haber-

407   Weiss-type reaction (*Fridovich, 1978*). Mn-SOD is considered as a general stress responsive factor

408   whose expression might be influenced by a variety of intracellular and environmental cues

409   including cold stress at transcriptional and/or translational levels (*Cho et al., 2006; Zelko et al.,*

410   *2002*). Only a little is known to date about oxidative stress induced by cold and functional

411   characterization of SOD in cold-hardy insects. In the present study, a *mMn-SOD* gene, *MpmMn-*

412   *SOD*, from the desert beetle *Microdera punctipennis* was cloned, characterized and the cold

413   protective effect of MpmMn-SOD protein was investigated for the first time.

414   Sequence analysis showed that *MpmMn-SOD* encodes four metal-binding residues (His26,

415   His76, Asp162, and His166) and a highly conserved Mn-SOD amino acid motif DI/VWEHAYY,

416   suggesting that these sites were essential to the structure and function of Mn-SODs. The

417   identification of the signature sequence and the conserved metal-binding residues suggested that

418   MpmMn-SOD possessed the essential properties of Mn-SOD family. Many mitochondrial proteins

419   are synthesized as precursors containing MTS. The finding of MTS in MpmMn-SOD sequence

420   suggested that MpmMn-SOD was of precursor type being transported into the mitochondria

421   (*Yamamoto et al., 2005c*).

422   A BLASTP search at GenBank revealed that MpmMn-SOD sequence was most close to

423   amino acid sequence of Mn-SOD from the yellow meal worm *T. molitor* with identity of 35.27%,

424   indicating that MpmMn-SOD was more diverged from the other Mn-SODs in insects.

425   Phylogenetic analysis confirmed this relationship. These two insects are belonging to the family

426   of Tenebrionidae (Coleoptera), their Mn-SOD sequences both were short at the N-terminal. The

427   close relationship of their Mn-SOD sequences may roughly reflect their taxonomic relationships.

428   The phylogenetic tree revealed that Mn-SOD and Cu/Zn-SOD may originate from a same ancestor,

429   and Mn-SOD may have evolved longer than Cu/Zn-SOD. Besides, Cu/Zn-SOD clade was

430   subdivided into ecCu/Zn-SOD and icCu/Zn-SOD, and ecCu/Zn-SOD subgroup showed more

431   divergency than icCu/Zn-SOD, these two protein sub-families may evolve by gene replication.

432   Previous study suggested that *Mn-SOD* in insect is widely distributed in a variety of cells and

433   tissues (*Zelko et al., 2002*). We found that *MpmMn-SOD* also distributes in all the tested tissues,

434   but the expression levels varied greatly among tissues, and the highest was in hindgut, followed

435   by in fat body. Thus, *MpmMn-SOD* may mainly function in hindgut and fat body. The hindgut

436   includes Malpighian tubule which plays an important role in detoxification and elimination of

437   toxins (*Beyenbach et al., 2010*). And fat body is one of the prime sites for antioxidant enzymes

438   (*Kwang Sik et al., 2005; Yamamoto et al., 2005a; Yamamoto et al., 2005b; Yamamoto et al.,*

439   *2005d*). Our result is similar to those on *Glossina morsitans* (*Munks et al., 2010*) and *Agrilus*

440   *planipennis* (*Swapna et al., 2011*), they both have significant SOD mRNA levels in fat body and

441   hindgut. The great up-regulation of *MpmMn-SOD* in hindgut and fat body, in turn, indicated that

442   these two tissues were important sites for resisting oxidative attack.

443   Mn-SOD has been considered a stress-responsive factor and its expression at the

444   transcriptional and translational levels might be influenced by a variety of intracellular and

445   environmental factors, including cold stress (*Fukuhara et al., 2002*). The *Mn-SOD* mRNA of the

446   fall webworm *Hyphantria cunea* (*Kim et al., 2010*) and the bee *Apis cerana* (*Jia et al., 2014*) were

447   highly increased at 4 ℃. Similar result is also reported in oriental fruit fly *Bactrocera dorsalis*

448   exposed to 0 ℃ (*Gao et al., 2013*). Our previous work found that *MpmMn-SOD* was one of the

449   eight significantly up-regulated genes related to abiotic stress response in the transcriptomic data

450   of the cold treated insects (*Tusong et al., 2017*). Here, we confirmed the expression profiling of

451 *MpmMn-SOD* at 4 ℃ for different time lengths to detect the responsive pattern of the gene to cold

452 stress. We found that *MpMn-SOD* mRNA levels were very sensitively modulated by 4 ℃ cold

453 stress. Within 0.5 h of 4 ℃ treatment, its expression increased to 9.9-fold of the control, and

454 reached to 125-fold of the control at 1.5 h, strongly indicating that cold stress stimulates the

455 expression of *MpmMn-SOD*. Our previous study on the *MpCu/Zn-SODs* showed that 4 ℃ stimulate

456 the expression of *MpecCu/Zn-SOD* but not *MpicCu/Zn-SOD* (*Xikeranmu et al., 2019*). Compared

457 with *MpecCu/Zn-SOD*, the *MpmMn-SOD* mRNA level was much higher than that of *MpecCu/Zn-*

458 *SOD* which was 6.8-fold of the control 4 ℃ for 0.5 h, implying that *MpmMn-SOD* may play major

459 role under cold stress. This was in consistent with the location of MpmMn-*SOD* in mitochondria,

460 where the electron-transport chain is responsible for a significant proportion of intracellular

461 superoxide radical production (*Møller, 2010*). The rapid increase of the *MpmMn-SOD* levels under

462 cold acclimation may reflect the adaptation of *M. punctipennis* to Guerbantonggut desert which is

463 characterized with rapid and large temperature fluctuation. Similar result was found in the

464 polychaete *Perinereis nuntia* treated with Cd (50 μg/L), in which *Mn-SOD* had a greater

465 susceptibility than *Cu/Zn-SOD* (*Won, 2014*). It is noticeable that the cold expression profile of

466 *MpmMn-SOD* under 4℃ presented as a stress-responsive type, which is characterized with drastic

467 fluctuation during the cold treatment period, the first and second large peaks appeared at 1.5 h and

468 11 h of the cold treatment, which were 125-fold and 67.3-fold of the control respectively. The

469 appearance of the second large peak looks like another round of cold defense is going on. These

470 results may be interpreted as the cells cold timely adjust the level of the enzyme to keep a relative

471 intracellular balance, because stress-responsive expression is at the cost of the inhibition of other

472 genes expression.   On the other hand, with the prolong of the cold stress, ROS increased again,

473 and cells need to produce more MpmMn-SOD to deal with the excessive ROS. Our previous work

474 (*Xikeranmu et al., 2019*) showed that there was a rapid increase of $O_2\bullet^-$ content in the beetle after

475 an exposure at 4 ℃ for 10 h, which is consistent with this result in this work.

476   The anti-oxidative activity of MpmMn-SOD was examined by investigating the involvement

477 of MpmMn-SOD in anti-oxidative stress by agar plate diffusion assay. The bacteria that

478 overexpressed MpmMn-SOD had significant smaller diameters of the inhibit zones on agar plates

479 than the control bacteria, demonstrating that MpmMn-SOD can significantly enhance cells

480 tolerance to H_2O_2-mediated oxidative stress. Jia et al (*Jia et al. 2014*) observed similar results with

481 ours, which shows the diameters of the death zones between the *Apis cerana* mMn-SOD-

482 overexpressing bacteria and the control bacteria are obviously different under oxidative stressors.

none
none

483 Our results showed that MpmMn-SOD indeed is an antioxidant enzyme that protect cells from
484 oxidative damage.

485   Overexpression of MpmMn-SOD in BL21(pET32a-mMn-SOD) showed significant
486 protective effect for the bacteria under cold stress, the survival curve of BL21(pET32a-mMn-SOD)
487 at -4 ℃ was a convex type, while it was almost a negative line for the control bacteria, suggesting
488 the cold resistance of BL21(pET32a-mMn-SOD) was significantly increased compared to the
489 control bacteria BL21(pET32a). Further, we determined the SOD activity and the $O_2\bullet^-$ content of
490 the transformed bacteria under -4 ℃ conditions. Within our expectations, the enzyme activity
491 during the cold treatment period was significantly higher than the control bacteria, and cold stress
492 could stimulate SOD activity of the bacteria cells. Correspondingly, the $O_2\bullet^-$ content was
493 significantly lower than the control during the cold treatment period, indicating that the
494 overexpression of MpmMn-SOD in *E. coli* cells enhanced cells ability to scavenge ROS thus to
495 reduce oxidative damage under cold conditions. The changing trends of the relative increase of
496 SOD activity and the relative decrease of $O_2\bullet^-$ content under cold stress was consistent, implying
497 the more increase in SOD activity, the more decrease in $O_2\bullet^-$ content. The low levels of these two
498 indexes at 4 h of cold treatment may due to a self-regulation of the cells to keep a relative
499 subcellular balance in SOD gene expression. However, we noticed that at 0h, the relative decrease
500 of $O_2\bullet^-$ content was roughly at the same level as at 2 h under cold conditions. This result may be
501 explained as BL21(pET32a-Mn-SOD) had higher SOD activity than the control and it functioned
502 well at room temperature.

503   Finally, we investigated the protective effect of MpmMn-SOD to BL21 (pET32a-mMn-SOD)
504 under -4 ℃ cold conditions. ROS accumulation can lead to membrane peroxidation and thus
505 destroy cell structure and function (*Mittler et al., 2004*). Thus, we measured relative electrolyte
506 leakage and MDA level in the bacteria cells. Within prediction, the plasma membrane leakage and
507 MDA contents in BL21 (pET32a-mMn-SOD) and BL21 (pET32a) both increased under -4 ℃ cold
508 stress, but the upward trend of the conductivity and MDA levels in BL21 (pET32a-mMn-SOD)
509 were significantly lower than the control bacteria (Fig.9). These results suggested that the damage
510 degree to cell membrane under cold stress to the transgenic bacteria was significantly less than in
511 control bacteria. Therefore, the high activity of MpmMn-SOD in the transformed bacteria should
512 play its role in eliminating ROS, and thus preventing the membrane lipids from peroxidation. The
513 present results agree with the work of Kwon et al (*Kwon et al., 2010*), who suggest that
514 overexpression of SOD induced tolerance to membrane damage.

Conclusions

516   In conclusion, the identified and characterized mitochondrial manganese superoxide
517 dismutase gene (*MpmMn-SOD*) from the desert beetle *Microdera punctipennis* was tissue-specific,
518 and cold inducible. It had anti-oxidative activity. The MpmMn-SOD overexpressed bacteria
519 treated at -4 ℃ showed increased cold resistance. Analysis of the SOD activity and $O_2\bullet^-$ content
520 in the MpmMn-SOD overexpressed bacteria treated at -4 ℃ revealed a significant negative
521 correlation, implying that MpmMn-SOD cold act as a defense mechanism to mitigate cell damage
522 caused by ROS under cold conditions. Accordingly, the MpmMn-SOD overexpressed bacteria
523 could decrease the plasma membrane damage caused by lipid peroxidation and kept better plasma
524 membrane integrity under cold stress. Our findings provide basic data for further study the
525 function, antioxidant mechanism and physiological responses of *Mn-SOD* gene in model species
526 exposed to temperature changes. Obviously, additional studies based on our data are needed to
527 gain further insights into the complex role of *Mn-SOD* gene in insect of cold tolerance.

Acknowledgements

529   We would like to acknowledge our fellow scholars, Fengjuan Zhang and Maimaitiaili
530 abudunasier for help collecting and identifying the insects used in this research.

Funding

532   The research was funded by the National Natural Science Foundation of China (No.
533 31360527), and Tianshan Cedar Project in 2017(2017xs20).

Competing Interests

535 The authors declare that they have no competing interests.

Author Contributions

537 Zilajiguli Xikeranmu, Xiaoning Liu and Ji Ma conceived and designed the study. Zilajiguli
538 Xikeranmu conducted all the experiments involved in this study. Zilajiguli Xikeranmu wrote the
539 paper with contributions from Xiaoning Liu and Ji Ma. All authors read and approved the final
540 version of the manuscript.

Data Availability

542 All data, models, and code generated or used during the study appear in the submitted article.

References

544 **Ackerman NB, Brinkley FB. 1966.** Oxygen tensions in normal and ischemic tissues during
545   hyperbaric therapy. Studies in rabbits. *Jama the Journal of the American Medical*
546   *Association* **198:**1280-1283 https://doi: 10.1001/jama.1966.03110250094027.
547 **Arenas-Ríos E, León-Galván MA, Mercado PE, López-Wilchis R, Cervantes DLMI, Rosado**
548   **A. 2007.** Superoxide dismutase, catalase, and glutathione peroxidase in the testis of the
549   Mexican big-eared bat (*Corynorhinus mexicanus*) during its annual reproductive cycle.
550   *Comparative Biochemistry & Physiology Part A Molecular & Integrative Physiology*
551   **148:**150-158 https:// doi:10.1016/j.cbpa.2007.04.003.
552 **Beyenbach K, Skaer H, and Dow J. 2010.** The Developmental, Molecular, and Transport
553   Biology of Malpighian Tubules. *Annual Review of Entomology* **55:**351-374 https://doi:
554   10.1146/annurev-ento-112408-085512.
555 **Bowler C. 1992.** Superoxide dismutase and stress tolerance. *Annurevplant Physiolplant Molbiol*
556   **43:**83-116 https://doi: 10.1146/annurev.arplant.43.1.83.
557 **Burmeister C, Lã¼Ersen K, Heinick A, Hussein A, Domagalski M, Walter RD, and Liebau**
558   **E. 2008.** Oxidative stress in *Caenorhabditis elegans*: protective effects of the Omega class
559   glutathione transferase (GSTO-1). *Faseb Journal* **22:**343-354 https:// doi: 10.1096/fj.06-
560   7426com.
561 **Chattopadhyay MK. 2002.** Low temperature and oxidative stress. *Current Science* **83:**109.
562 **Cho YS, Choi BN, Kim KH, Kim SK, Dong SK, Bang IC, Nam YK. 2006.** Differential
563   expression of Cu/Zn superoxide dismutase mRNA during exposures to heavy metals in
564   rockbream (*Oplegnathus fasciatus*). *Aquaculture* **253:**667-679 https://
565   doi:10.1016/j.aquaculture.2005.05.047.
566 **Denlinger DL. 2010.** Low temperature biology of insects. *Cambridge University Press*.
567   https://doi.org/10.1017/CBO9780511675997.
568 **Felton GW, Summers CB. 1995.** Antioxidant systems in insects. *Archives of Insect*
569   *Biochemistry and Physiology.* **29(2):**187-197 https://doi. 10.1002/arch.940290208.
570 **Fridovich I. 1978.** The biology of oxygen radicals. *Science* 201:875-880 https://
571   doi:10.1126/science.210504.
572 **Fukuhara R, Tezuka T, Kageyama T. 2002.** Structure, molecular evolution, and gene expression
573   of primate superoxide dismutases. *Gene* **296:**99-109 https:// doi:10.1016/s0378-
574   1119(02)00837-5.
575 **Gao XL, Li JM, Wang YL, Jiu M, Yan GH, Liu SS, Wang XW. 2013.** Cloning, expression and
576   characterization of mitochondrial manganese superoxide dismutase from the Whitefly,
577   *Bemisia tabaci. International Journal of Molecular Sciences* **14:**871-887 https://
578   doi:10.3390/ijms14010871.
579 **Gao XM, Jia FX, Shen GM, Jiang HQ, Dou W, Wang JJ. 2013.** Involvement of superoxide
580   dismutase in oxidative stress in the oriental fruit fly, *Bactrocera dorsalis*: molecular
581   cloning and expression profiles. *Pest Management Science* **69:**1315-1325 https://doi:
582   10.1002/ps.3503
583 **Gharari Z, Nejad RAK, Shekasteband R, Najafi F, Nabiuni M, Irian S. 2014.** The role of *Mn-*
584   *SOD* and *Fe-SOD* genes in the response to low temperature in chs mutants of *Arabidopsis*.

585   *Doga Turkish Journal of Botany* **38:**80-88 https:// doi:10.3390/ijms14010871.

586   **Harari PM, Fuller DJM, Gerner EW. 1989.** Heat shock stimulates polyamine oxidation by two
587   distinct mechanisms in mammalian cell cultures. *International Journal of Radiation*
588   *Oncology Biology Physics* **16:**451-457 https:// doi:10.1016/0360-3016(89)90341-6.

589   **Hermes-Lima M, Storey JM, Storey KB. 2001.** Chapter 20 Antioxidant defenses and animal
590   adaptation to oxygen availability during environmental stress. *Cell & Molecular Response*
591   *to Stress* **2:**263-287 https://doi.org/10.1016/S1568-1254(01)80022-X.

592   **Hou F, Ma J, Liu X, Wang Y, Liu XN, Zhang FC. 2010.** Seasonal changes in antifreeze protein
593   gene transcription and water content of beetle *Microdera punctipennis* (Coleoptera,
594   Tenebrionidae) from Gurbantonggut desert in Central Asia. *Cryo Letters* **31:**359-370
595   https://doi:10.1016/S1568-1254(01)80022-X.

596   **Huang RX, Hong-Ying HU, Wei WU, Fan ZT, Suo FY. 2005.** Formation and Evolution of
597   Desert Insects in Xinjiang and Its Adjacent Regions. *Arid Land Geography*. **28(1) :** 38-44
598   https://doi.10.13826/j.cnki.cn65-1103/x.2005.01.008

599   **Jaramillo-Gutierrez G, Molina-Cruz A, Kumar S, and Barillas-Mury C. 2010.** The Anopheles
600   gambiae oxidation resistance 1 (*OXR1*) gene regulates expression of enzymes that detoxify
601   reactive oxygen species. *Plos One* **5:**e11168 https:// doi:10.1371/journal.pone.0011168
602   https://doi: 10.1007/s00299-006-0127-4

603   **Jia H, Sun R, Shi W, Yan Y, Li H, Guo X, Xu B. 2014.** Characterization of a mitochondrial
604   manganese superoxide dismutase gene from *Apis cerana cerana* and its role in oxidative
605   stress. *Journal of Insect Physiology* **60:**68-79 https://doi:10.1007/s12562-011-0334-y

606   **Jithesh MN, Prashanth SR, Sivaprakash KR,Parida A. 2006.** Monitoring expression profiles
607   of antioxidant genes to salinity, iron, oxidative, light and hyperosmotic stresses in the
608   highly salt tolerant grey mangrove, *Avicennia marina* (Forsk.) Vierh. by mRNA analysis.
609   *Plant Cell Reports* **25:**865-876 https://doi: 10.1007/s00299-006-0127-4.

610   **Kailasam M, Kaneko G, Oo AKS, Ozaki Y, Thirunavukkarasu AR, Watabe S. 2011.** Effects
611   of calorie restriction on the expression of manganese superoxide dismutase and catalase
612   under oxidative stress conditions in the rotifer *Brachionus plicatilis*. *Fisheries Science*
613   **77:**403-409 https://doi:10.1007/s12562-011-0334-y.

614   **Kim YI, Kim HJ, Kwon YM, Kang YJ, Lee IH, Jin BR, Han YS, Cheon HM, Ha NG, Seo**
615   **SJ. 2010.** Modulation of MnSOD protein in response to different experimental stimulation
616   in *Hyphantria cunea*. *Comparative Biochemistry & Physiology Part B Biochemistry &*
617   *Molecular Biology* **157:**343-350 https:// doi:10.1016/j.cbpb.2010.08.003.

618   **Kwang Sik L, Seong Ryul K, Nam Sook P, Iksoo K, Pil Dong K, Bong Hee S, Kwang Ho C,**
619   **Seok Woo K, Yeon Ho J,Mong LS. 2005.** Characterization of a silkworm thioredoxin
620   peroxidase that is induced by external temperature stimulus and viral infection. *Insect*
621   *Biochemistry and Molecular Biology* **35:**73-84 https:// doi:10.1016/j.ibmb.2004.09.008.

622   **Kwon SY, Jeong YJ, Lee HS, Kim JS, Cho KY, Allen RD, Kwak SS. 2010.** Enhanced
623   tolerances of transgenic tobacco plants expressing both superoxide dismutase and
624   ascorbate peroxidase in chloroplasts against methyl viologen-mediated oxidative stress.
625   *Plant Cell & Environment* **25:**873-882 https:// doi:10.1046/j.1365-3040.2002.00870.x.

626 **Li C, He J, Su X, Li T. 2011.** A manganese superoxide dismutase in blood clam *Tegillarca*
627   *granosa* : Molecular cloning, tissue distribution and expression analysis. *Comparative*
628   *Biochemistry & Physiology Part B Biochemistry & Molecular Biology* **159:**64-70
629   https://doi:10.1016/j.cbpb.2011.02.003
630 **Lin YC, Lee FF, Wu CL, Chen JC. 2010.** Molecular cloning and characterization of a cytosolic
631   manganese superoxide dismutase (cytMnSOD) and mitochondrial manganese superoxide
632   dismutase (mtMnSOD) from the kuruma shrimp *Marsupenaeus japonicus*. *Fish &*
633   *Shellfish Immunology* **28:**143-150 https://doi:10.1016/j.fsi.2009.10.012.
634 **Liu YC, Su H, Wang PC, Xu YL, Wei TC, Wang HB, Xu YS. 2018.** Cloning,Fusion
635   Expression and Enzyme Activity Analysis of Extracellular Copper Zinc Superoxide
636   Dismutase in Mulberry Pyralid,*Glyphodes pyloalis*. *Science of Sericulture* **44(2):** 0188-
637   0195 https:// doi: 10.13441/j.cnki.cykx.2018.02.002.
638 **McCord JM, Fridovich I. 1988.** Superoxide dismutase: The first twenty years (1968–1988). *Free*
639   *Radical Biology Medicine* **5:**363-369 https:// doi:10.1016/0891-5849(88)90109-8.
640 **Meng Q, Jing C, Xu C, Huang Y, Wang Y, Wang T, Zhai X, Wei G, Wen W. 2013.** The
641   characterization, expression and activity analysis of superoxide dismutases (SODs) from
642   *Procambarus   clarkii.   Aquaculture   **406:**131-140   https://
643   doi:10.1016/j.aquaculture.2013.05.008.
644 **Mittler R, Vanderauwera S, Gollery M, Breusegem FV. 2004.** Reactive oxygen gene network
645   of plants. *Trends in Plant Science* **9:**490-498 https:// doi: 10.1016/j.tplants.2004.08.009.
646 **Møller IM. 2010.** ROS signaling—specificity is required. *Trends Plant Science* **15(7):**370-374
647   https:// doi:10.1016/j.tplants.2010.04.008.
648 **Munks RJ, Sant'Anna MR, Grail W, Gibson W, Igglesden T, Yoshiyama M, Lehane SM,**
649   **Lehane MJ. 2010.** Antioxidant gene expression in the blood-feeding fly *Glossina*
650   *morsitans morsitans*. *Insect Molecular Biology* **14:**483-491 https:// doi:10.1111/j.1365-
651   2583.2005.00579.x
652 **Park SY KY, Yang DJ, Yoo MA. 2004.** Transcriptional regulation of the *Drosophila* catalase
653   gene by the DRE/DREF system. *Nucleic Acids Research* **32(4):**1318-1324. https://
654   doi:10.1093/nar/gkh302.
655 **Rauen U, Polzar B, Stephan H, Mannherz HG, Groot HD. 1999.** Cold-induced apoptosis in
656   cultured hepatocytes and liver endothelial cells: mediation by reactive oxygen species.
657   *Faseb Journal* **13:**155-168 https:// doi:10.1096/fasebj.13.1.155.
658 **Sarvajeet Singh G,Narendra T. 2010.** Reactive oxygen species and antioxidant machinery in
659   abiotic stress tolerance in crop plants. *Plant Physiology Biochemistry* **48:**909-930 https://
660   doi: 10.1016/j.plaphy.2010.08.016.
661 **Schafer FQ, Buettner GR. 2001.** Redox environment of the cells as viewed through the redox
662   state of the glutathione disulfide/glutathione couple. *Free Radical Biology and Medicine*
663   **30:**1191-1212 https:// doi: 10.1016/S0891-5849(01)00480-4.
664 **Swapna Priya R, Praveen M, Herms DA, Pierluigi B, Omprakash M. 2011.** Antioxidant genes
665   of the emerald ash borer (*Agrilus planipennis*): gene characterization and expression
666   profiles.   *Journal   of   Insect   Physiology*   **57:**819-824   https://   doi:

667   10.1016/j.jinsphys.2011.03.017.

668 **Tusong K, Guo XX, Meng S, Liu XN, Ma J. 2017.** Comparative analysis of the transcriptome
669   of the overwintering desert beetle *Microdera punctipennis*. *Cryobiology* **78:**80-89 https://
670   doi:10.1016/j.cryobiol.2017.06.009.

671 **Tusong K, Liu XY, Liu XN, Ma J. 2016.** Transcriptomic analysis of the desert beetle *Microdera*
672   *punctipennis*(Coleoptera: Tenebrionidae) in response to short-term cold stress. *Acta*
673   *Entomologica Sinica*. **59(6):**581-591  https://doi:10.16380/j.kcxb.2016.06.001.

674 **Vaughan M. 1997.** Oxidative Modification of Macromolecules Minireview Series. *Journal of*
675   *Biological Chemistry* **272:**18513-18513 https:// doi:10.1074/jbc.272.30.18513.

676 **Wang AG, Luo GH. 1990.** Quantitative Relation between the Reaction of Hydroxylamine and
677   Superoxide Anion Radicals in Plants. *Plant Physiology Communications*. **6:**55-57. https://
678   doi:10.13592 /j.cnki.ppj.1990.06.031.

679 **Won EJ, Ra K, Kim KT, Lee JS, Lee YM. 2014.** Three novel superoxide dismutase genes
680   identified in the marine polychaete *Perinereis nuntia* and their differential responses to
681   single and combined metal exposures. *Ecotoxicology and Environmental Safety* **107:**36-45
682   https:// doi:10.1016/j.ecoenv.2014.03.026.

683 **Xikeranmu Z, Abdunasir M, Ma J, Tusong K, and Liu XN. 2019.** Characterization of two
684   copper/zinc superoxide dismutases (Cu/Zn-SODs) from the desert beetle *Microdera*
685   *punctipennis* and their activities in protecting *E. coli* cells against cold. *Cryobiology* **87:**
686   15-27. https:// doi:10.1016/j.cryobiol.2019.03.006.

687 **Yamamoto K, Banno Y, Fujii H, Miake F, Kashige N, Aso Y. 2005a.** Catalase from the
688   silkworm, *Bombyx mori* : Gene sequence, distribution, and overexpression. *Insect*
689   *Biochemistry & Molecular Biology* **35:**277-283 https:// doi:10.1016/j.ibmb.2005.01.001.

690 **Yamamoto K, Zhang P, Banno Y, Fujii H, Miake F, Kashige N, Aso Y. 2005b.** Superoxide
691   Dismutase from the Silkworm,*Bombyx mori*:Sequence,Distribution,and Overexpression.
692   *Journal of the Agricultural Chemical Society of Japan* **69:**507-514 https:// doi:
693   10.1271/bbb.69.507.

694 **Yamamoto K, Zhang P, He N, Wang Y, Aso Y, Banno Y,Fujii H. 2005c.** Molecular and
695   biochemical characterization of manganese-containing superoxide dismutase from the
696   silkworm, *Bombyx mori*. *Comparative Biochemistry & Physiology Part B Biochemistry &*
697   *Molecular Biology* **142:**403-409 https:// doi:10.1016/j.cbpb.2005.09.002.

698 **Yamamoto K, Zhang P, Miake F, Kashige N, Aso Y, Banno Y, Fujii H. 2005d.** Cloning,
699   expression and characterization of theta-class glutathione S -transferase from the silkworm,
700   *Bombyx mori*. *Comparative Biochemistry & Physiology Part B Biochemistry*

701 **Zelko IN, Mariani TJ, Folz RJ. 2002.** Superoxide dismutase multigene family: a comparison of
702   the *CuZn-SOD (SOD1)*, *Mn-SOD (SOD2)*, and *EC-SOD (SOD3)* gene structures,
703   evolution, and expression. *Free Radical Biology Medicine* **33:**337-349
704   https://doi:10.1016/S0891-5849(02)00905.

705

Figure 1

Fig 1. Nucleotide and deduced amino acid sequences of a Mn-SOD from the beetle *M. punctipennis*. The letters in box indicate the start codon (ATG) and the stop codon (TAA). The putative mitochondrial targeting sequence (MTS) is underlined in black. T

The letters in box indicate the start codon (ATG) and the stop codon (TAA). The putative mitochondrial targeting sequence (MTS) is underlined in black. The putative polyadenylation signal (AATAAA) and poly A are underlined in blue. The potential N-glycosylation site is shown in pink (NGTL). The Mn-SOD signature motif (DIWEHAYY) is highlighted in cyan. The four highly conserved amino acids (His26, His76, Asp162, and His166) critical for Mn-binding are circled in red.

```
1    ATGTTTAAATTACCAAAATTACCTTATTCCTTTAATGCTTTAGCTCCACGTATATCTGCA
1     M  F  K  L  P  K  L  P  Y  S  F  N  A  L  A  P  R  I  S  A

61   GAAACATTACAGTTTCATTACAGTAAACATCATGCTGCATATGTAAATAAATTGAATGAA
21    E  T  L  Q  F  Ⓗ  Y  S  K  H  H  A  A  Y  V  N  K  L  N  E

121  ATTTTAAGAGACAAAAAGAGTAAGGATCAACCAAAATCTCTTTTGGAAATTATAAGAAAA
41    I  L  R  D  K  K  S  K  D  Q  P  K  S  L  L  E  I  I  R  K

181  GAAAATAATGGGACATTATTCAATCAAGCAGCTCAATCGTGGAATCATGAATTTTACTGG
61    E  N  N̲ ̲G̲ ̲T̲ ̲L̲  F  N  Q  A  A  Q  S  W  N  Ⓗ  E  F  Y  W

241  AATTGTCTAACCCCAAATGGAGGAGGTAAACCATACGGACTAGTACAAACATTAATTGAG
81    N  C  L  T  P  N  G  G  G  K  P  Y  G  L  V  Q  T  L  I  E

301  CGTGACTATCAAGATTTTGATACGTTTAAAAATCAATTTACAAGTGCAGCATCCACGCAT
101   R  D  Y  Q  D  F  D  T  F  K  N  Q  F  T  S  A  A  S  T  H

361  TTTGGTTCAGGATGGGTATGGTTATGTTTTAATAAAGAAAGTGGAAAACTTGAGATCCAA
121   F  G  S  G  W  V  W  L  C  F  N  K  E  S  G  K  L  E  I  Q

421  CAAACACATGATGCCCAACATCCAATTAAATTAAATTCTAATTTGGTGCCAATATTGACT
141   Q  T  H  D  A  Q  H  P  I  K  L  N  S  N  L  V  P  I  L  T

481  TGTGACATTTGGGAACATGCTTATTATATAGACTATAGAAATGCTCGACCAAAATATATA
161   C  Ⓓ  I  W  E  Ⓗ  A  Y  Y  I  D  Y  R  N  A  R  P  K  Y  I

541  CAAGCTTGGTGGGATACATTGAACTGGAATTTTGCTAATTTATGTTTGGAAAAAAAATCC
181   Q  A  W  W  D  T  L  N  W  N  F  A  N  L  C  L  E  K  K  S

601  GTCGACTAAGAGTTAATATAAATTTTTTTCTTTTTTGCTTTTTTCTATCTGCATGCAACG
201   V  D  *

661  CTGAAATTAGTCAACAAATAAGCTATTTTTTTCATTATATAATTTTTATAGATAACCAAC

721  TTTTTTAACAATTCTAGAAACAAATGGTTTTTGAATTAGCAAAATTACCTTTTAGCGAAG

781  ATGCGCTTAAACCGCATATATCCCCTCAAACATTACAATTTCATCATGGCAAACATCATG

841  CGTCATATGTTAATAATTTGAACAATCTAACTAAAGGGACACCAATGGAACGCTTAAGCT

901  TACAAGATGTTGTCATCCAAGCTGAAGGTGCAACATTTAACCAAGCGGCACAAGCATGGA

961  ATCATGATTTTTATTGGCAATCTTTAACCCCGTCTCAATCTGGTGGACCAATAGGAGAGC

1021 TTAAACAAATGATAGAAGCAGAATTTGGAAATTTTGATGAATTTAAAAGTAAGTTTTCTA

1081 GTGCAGCTTCAGGACATTTTGGCTCCGGATGGGCATGGCTTGTCTATGATACTAAACAAA

1141 ATAAAGTTAAAATACATCAAACACATGACGCAGGAAATCCATTAAAGGATGGAGCTGGAA

1201 TTCCACTATTGACATGTGATGTATGGGAACATGCATATTATCTCGATTATCAGAATAATA

1261 GAGCTCAATATATTGACGCTTGGTGGAAAATAGCCAATTGGAAATTTGCAGAAGAAATT

1316    TAAGAAAGTGCTTGAAAAAAATAAACTATTAAAAAAAAAA
```

Figure 2

Fig 2. Multiple alignments of the deduced amino acid sequences of the Mn-SODs from the beetle *M. punctipennis* and other known insect species. The Mn-SOD signature DIWEHAYY is boxed in red (labeled Signature). Mn-binding sites are indicated with tria

The Mn-SOD signature DIWEHAYY is boxed in red (labeled Signature). Mn-binding sites are indicated with triangles. The amino acid homology up to 100% is shown in black, 75% ~99% is in pink and 50% ~74% in cyan. *M. punctipennis*: *Microdera punctipennis; T. molitor: Tenebrio molitor; A. mellifera*: *Apis mellifera; B.tabaci: Bemisia tabaci; H.armigera: Helicoverpa armigera; T. castaneum: Tribolium castaneum.*

MTS

M.punctipennis	..........................MFKLEKLFYSFNALAERISAETLQFHYSKHH	31
T.molitor	.........................MHTLEDLFYDYDALEPVISSEIMKIHHAKHH	31
A.mellifera	MFAARRILFSNTVKDTFTR.........TKHTLEDLFYDYKALEPIISAEIMQLHHSKHH	51
B.tabaci	MFACSK.KIASSLASSRTCMNVVNRSMSDKATLEKLFFGYKDLEPVISGEIMELHHSKHH	59
H.armigera	MFAKRRFLLTSAVNAVR..........QKHTLEELFYEYSALEPVISREIMSLHHSKHH	49
T.castaneum	MFALRR.LATAPLAGSR..........AAHSLEELFYAYEALEPVISRDIMCLHHSKHH	48
Consensus	lp lp l p is h khh	

M.punctipennis	AAYVNKLNEILRDKKSKDQPKSLLEIIRKENNGTLFNQAAQSWNEEFYWNGITPN...GG	88
T.molitor	KAYVDNLNKAEEGLQKALSEKDVSSQIAFHN.ALKFNGGGHLNESIFWNNLAPKSRGGG	89
A.mellifera	ATYVNNLNVAEEKMKEAVAKGDVNTQVALSP..AIKFNGGGHLNESIFWCNLSPN....G	105
B.tabaci	AAYVTNYNVALEKLQEATAKNDANAIVTLGP..ALKFNGGGHINESIFWTVLSKD....G	113
H.armigera	ATYINNLNAEEEKLAQAQAKGDISTVISLAP..GLKFNGGGHINETIFWQNLSPN....G	103
T.castaneum	QTYVTNLNAAEEKLKAALSKGDISTAISLEP..ALRFNGGGHLNESIFWQNLSPE....S	102
Consensus	y n nh w l	

M.punctipennis	GKPYGLVQTLIERDYQDFDTFKNQFTSAASTHFGSGWVWLCFNKESGKIEIQQTHDACHP	148
T.molitor	YLNNGQLKTQIEKQFSSFAKFKEVFSSQAVAIKGSGWAWLGYDTRTKNLALATCQN.QDP	148
A.mellifera	GKPDAALLNQIKKDFGSIEEMKKRLSENTIAIQGSGWGWLGYCQKSKSLRIATCAN.QDP	164
B.tabaci	GKPSDDLLAAINRDFGSLDNLKTQLQTASNGVQGSGWGWLGINSQTKKLQVTTTAN.QDP	172
H.armigera	GKPSGSLTQAIEKDFGSWDNMKNQLAAASVGVQGSGWGWLGYNKQMKKLQIAPSQN.QDP	162
T.castaneum	TQPSDALKKAIEDSFGGVQQLKDQLSASSIGVQGSGWGWLGYCSKSGKIKIATCAN.QDP	161
Consensus	i k gsgw wl l q p	

M.punctipennis	IKLNSNLVPILTCDIWEHAYYIDYRNARPKYIQAWWDTLNWNFANLCLEKKSVD.	202
T.molitor	LLATVGLIPLLGVDVWEHAYYLQYKNERPKYVDAIWEIVNWKNVEESYQKAVEFS	203
A.mellifera	LQATTGLIPLFGIDVWEHAYYLQYKNVRPDYVKAIFDVVNWNDVNSRYKKAIGS.	218
B.tabaci	LQATTGLIPLFGIDVWEHAYYLQYKNVRPSYTKAILDIVNWSEVSRRYSAAV...	224
H.armigera	LQATTGLIPLFGIDVWEHAYYLQYKNARADYVKAIFDVANWGDVSKRFEAAVN..	215
T.castaneum	LQATTGLVPLLGIDVWEHAYYLQYKNVRADYVKAIFEIVNWKDVSQRFEKAKSC.	215
Consensus	l p d wehayy y nr y a nw	

Signature

Figure 3

Fig 3. Phylogenetic analysis of SOD sequences from *M. punctipennis* and other insect species based on predicted amino acid sequences. [i]A.cerana cerana: Apis cerana cerana; A. glabripennis: Anoplophora glabripennis; A. planipennis: Agrilus planipenn

A.cerana cerana: Apis cerana cerana; A. glabripennis: Anoplophora glabripennis; A. planipennis: Agrilus planipennis; A.rosae: Athalia rosae; A. tumida: Aethina tumida; B.mori: Bombyx mori; B.tabaci: Bemisia tabaci; C.formosanus: Coptotermes formosanus; C. lapponica: Chrysomela lapponica. D. helophoroides: Dastarcus helophoroides; D.melanogaster: Drosophila melanogaster; D.plexippus: Danaus plexippus; G.morsitans morsitans: Glossina morsitans morsitans; H.saltator: Harpegnathos saltator; M. punctipennis: Microdera punctipennis; O.biroi: Ooceraea biroi; P. coochleariae: Phaedon cochleariae; T. castaneum: Tribolium castaneum; T. molitor: Tenebrio molitor; Z. nevadensis: Zootermopsis nevadensis.
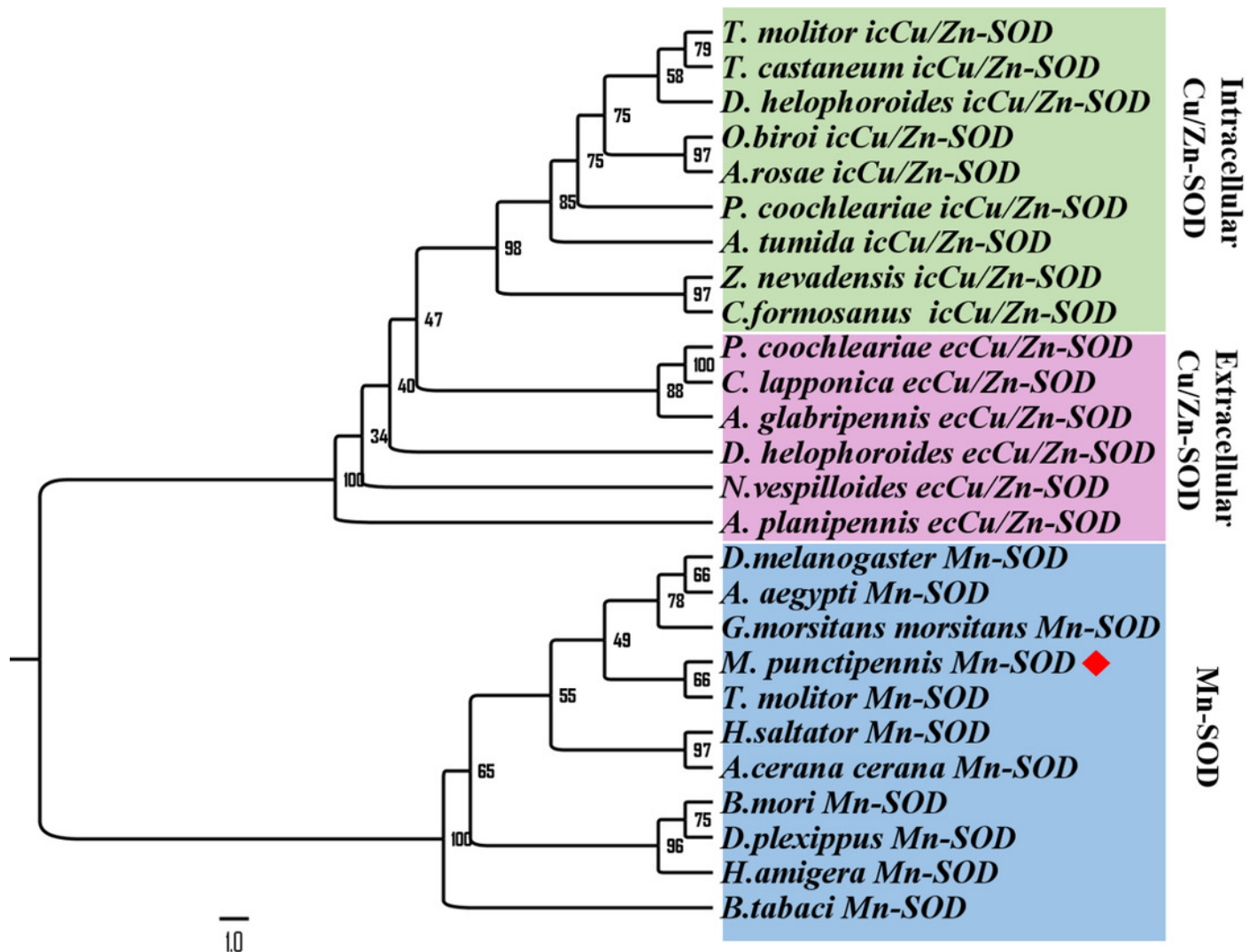
Figure 4

Fig 4. Relative mRNA levels of *MpmMn-SOD* gene detected by RT-qPCR. (A) The
expression profile of *MpmMn-SOD* gene in different tissues. Values are represented as
fold change compared to that of the head; (B) Temporal expression of [i]MpmMn-SOD[i

(A) The expression profile of *MpmMn-SOD* gene in different tissues. Values are represented
as fold change compared to that of the head; (B) Temporal expression of *MpmMn-SOD* gene
under 4 ℃ cold stress. Values are represented as fold change compared to the control (0 h).
Different letters above each column indicate statistical significance. *P<0.05* (lower-case
letters), *P<0.01*(capital letters).
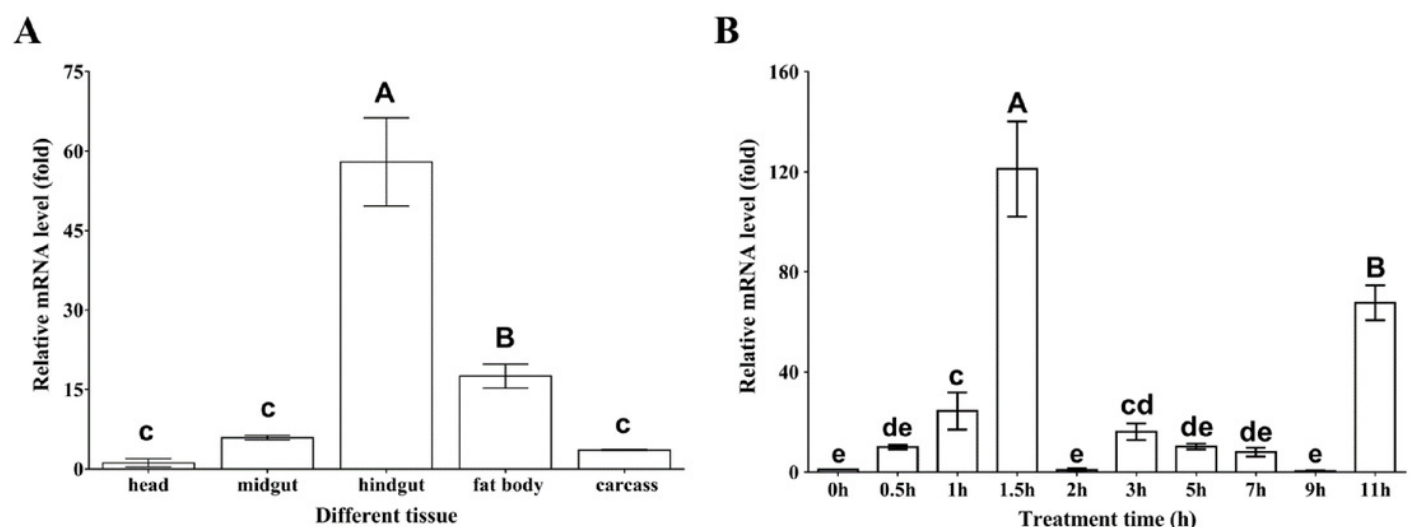
Figure 5

Fig 5. Analysis of the fusion protein Trx-His-mMpMn-SOD overexpressed in BL21 cells. (A) SDS-PAGE analysis of the whole cell lysate. (B) Western blot analysis. M: protein marker; lane1: non-induced BL21(pET32a); lane2: induced BL21(pET32a); lane3: un-indu

(A) SDS-PAGE analysis of the whole cell lysate. (B) Western blot analysis. M: protein marker;

lane1: non-induced BL21(pET32a); lane2: induced BL21(pET32a); lane3: un-induced

BL21(pET32a-mMn-SOD); lane4: induced BL21 (pET32a-mMn-SOD).
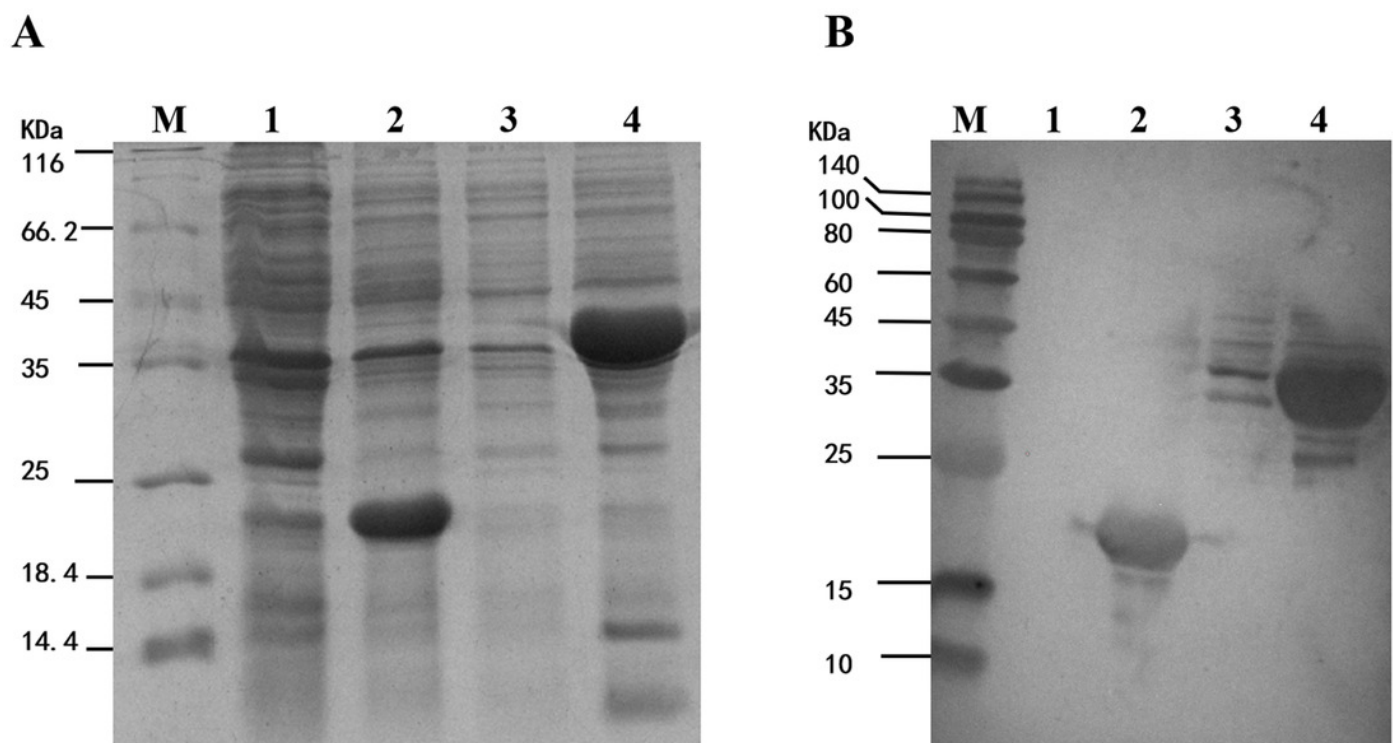
Figure 6

Fig 6. Antioxidant activity assay on LB agar plates containing *E. coli* cells overexpressing MpmMn-SOD. Oxford cups containing different concentrations of H_2O_2 were used to generate oxidative stress to the cells. (A) Inhibited zon

Oxford cups containing different concentrations of H_2O_2 were used to generate oxidative

stress to the cells. (A) Inhibited zones of the bacteria on agar plates. Numbers 1~4 on each

disc represents different H_2O_2 concentrations from 100 mM to 25 mM. mMn-SOD: *E. coli* cells

BL21(pET32a-mMn-SOD); Control: *E. coli* cells BL21(pET32a). (B) Quantitative diameters of

the inhibited zones in histograms. Values are compared to the control bacteria between the

same group. The data are the mean ± *S.E*. of three replicate.
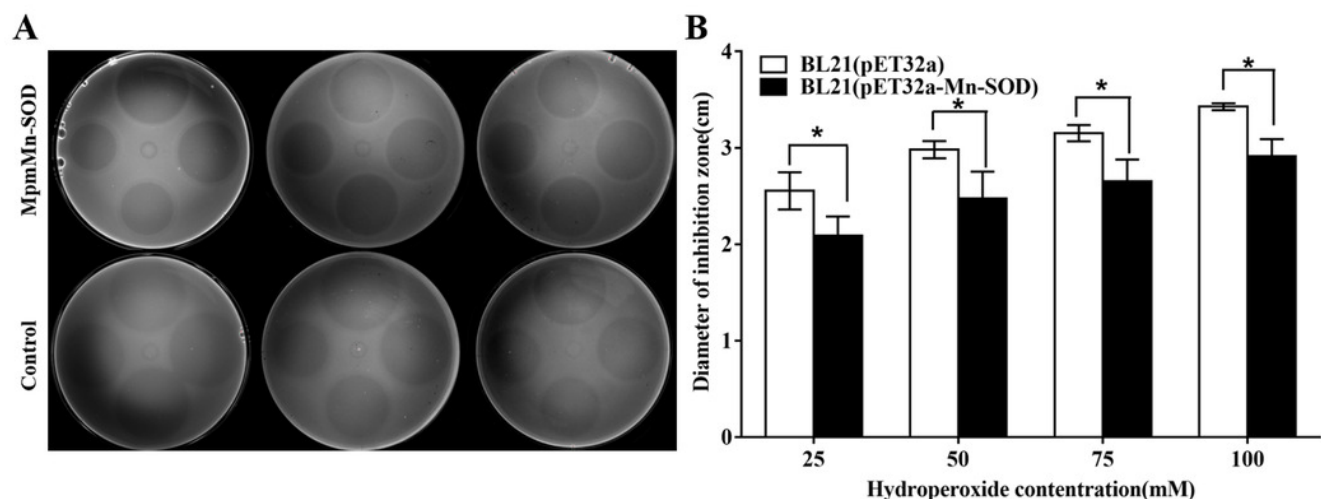
Figure 7

Fig.7. Survival curve of the MpmMn-SOD overexpressed BL21 (pET32a-mMn-SOD) at -4 ℃
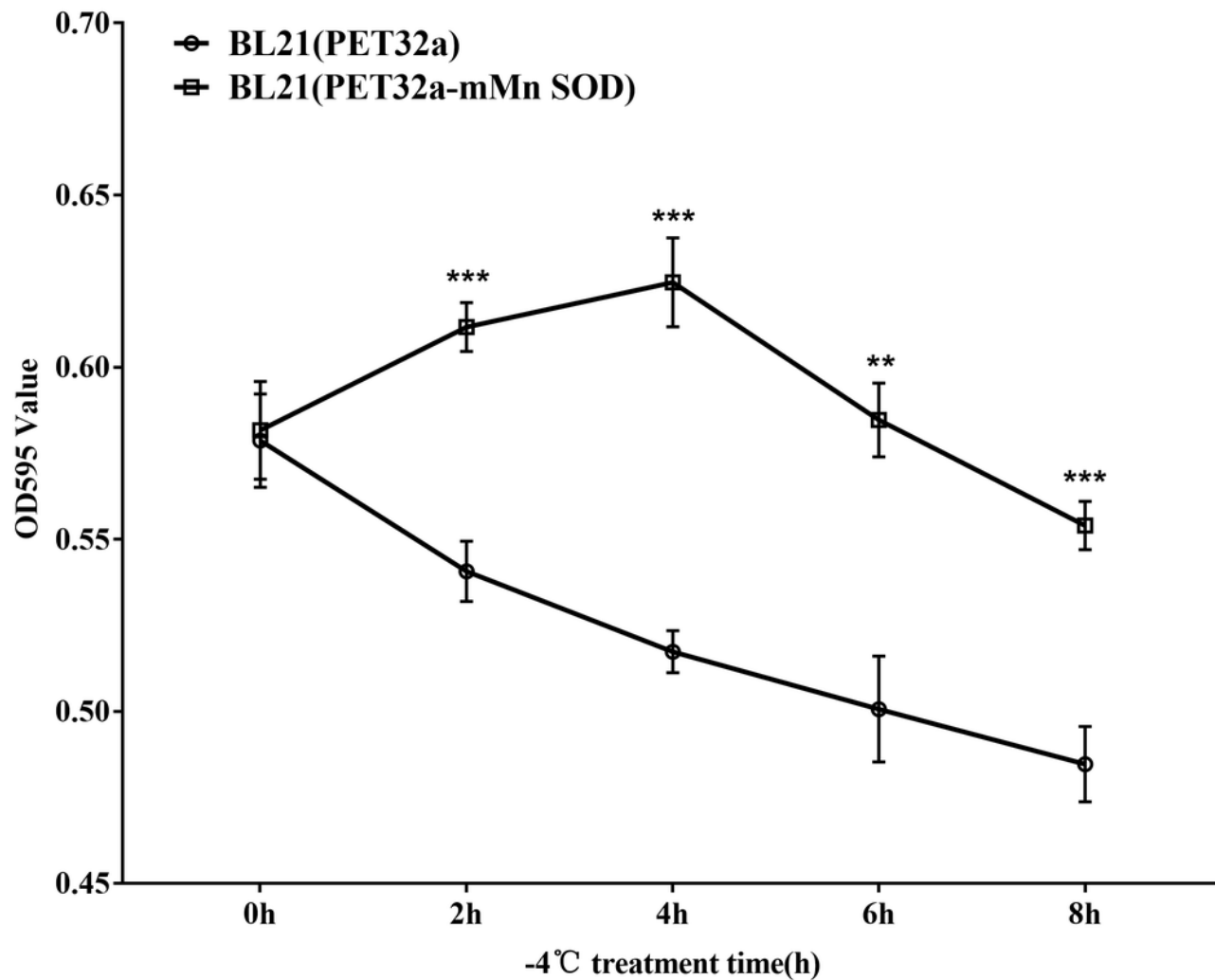
Figure 8

Fig. 8. SOD activity and $O_2\bullet^-$ content in bacteria BL21 in response to -4 °C cold stress.

(A) SOD activity in bacteria BL21 (pET32a) and (pET32a-mMn-SOD). (B) $O_2\bullet^-$ content in bacteria BL21 (pET32a) and (pET32a-mMn-SO

(A) SOD activity in bacteria BL21 (pET32a) and (pET32a-mMn-SOD). (B) $O_2\bullet^-$ content in bacteria BL21 (pET32a) and (pET32a-mMn-SOD). (C) Relative increase in SOD activity. (D) Relative decrease in $O_2\bullet^-$ content. Different letters over each column indicate statistical significance, $P < 0.05$.
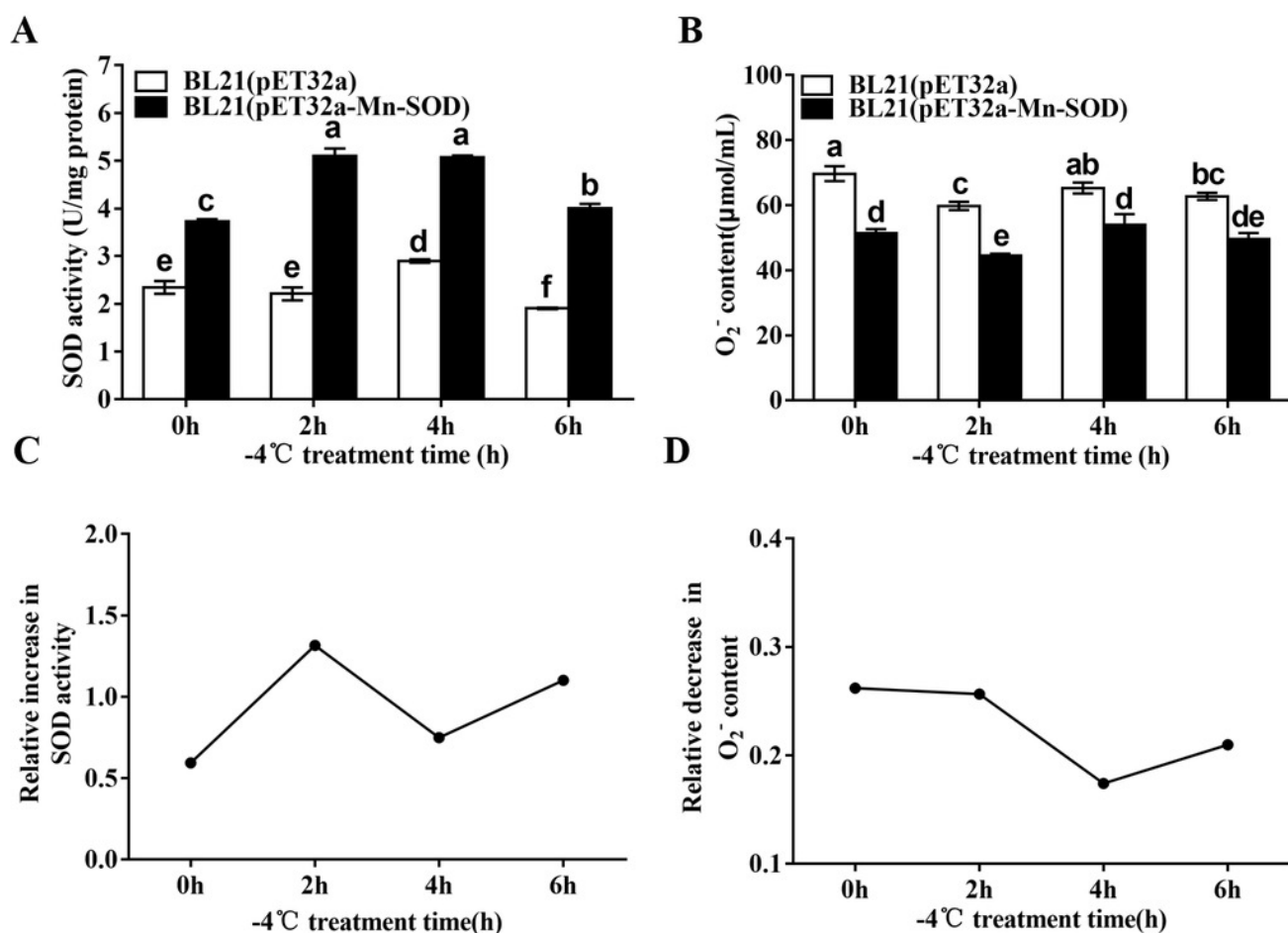
Figure 9

Fig 9. Protective effect of MpmMn-SOD on bacteria BL21(pET32a-mMn-SOD) in response to -4 °C cold stress. (A) Relative conductivity of BL21(pET32a-mMn-SOD) and BL21(pET32a) under -4 ℃. (B) MDA content of BL21 (pET32a-mMn-SOD) and BL21 (pET32a) under -4 ℃.

(A) Relative conductivity of BL21(pET32a-mMn-SOD) and BL21(pET32a) under -4 ℃. (B) MDA content of BL21 (pET32a-mMn-SOD) and BL21 (pET32a) under -4 ℃. Paired t-test was conducted to analyze the difference between BL21 (pET32a-mMn-SOD) and BL21 (pET32a) at each time treatment group. The symbol * indicates statistical significance $P < 0.05$. Values are expressed as means ±S.E. (n=3).
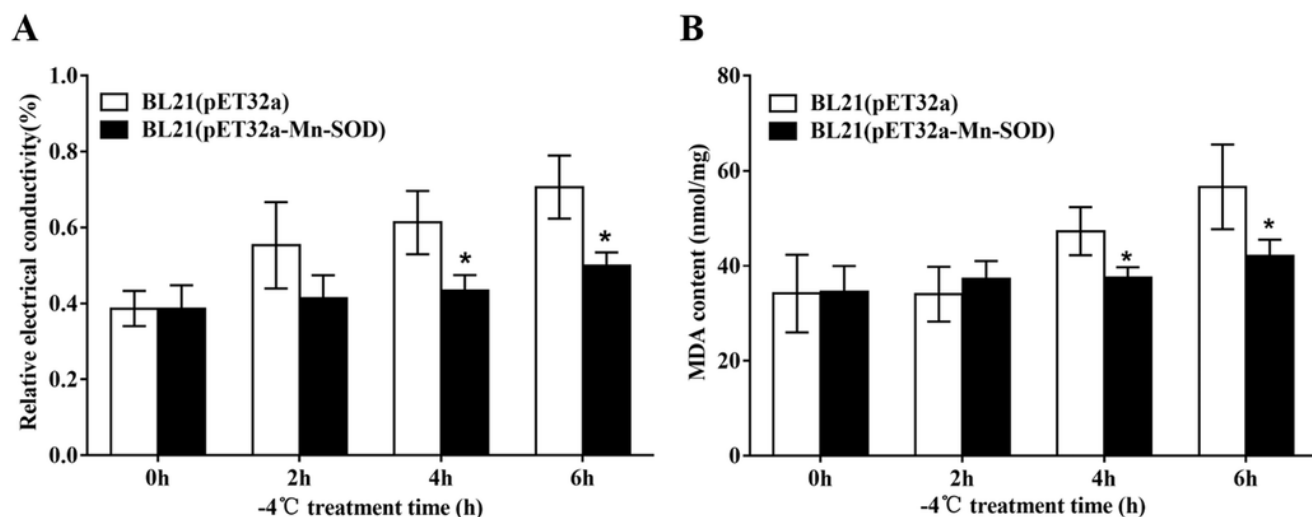
Table 1 Primer sequences used in this study

1   Table 1   Primer sequences used in this study

Primer name	Primer sequence (5'→3')	Description
Primers for RACE		
Mp MnSOD-F1	TCGAAGTGTTGTTGGACGGGCTATC	3'- RACE first round PCR
Mp MnSOD-F2	CCCTAGCTTGTGGCGTTATCGCTTA	3'- RACE second round PCR
Universal Primer A Mix (UPM)	CTAATACGACTCACTATAGGGCAAGC AGTGGTATCAACGCAGAGT	3' ,5'-RACE first round PCR
Universal Primer Short	AAGCAGTGGTATCAACGCAGAGT	3' ,5'-RACE second round PCR
Primers for qRT-PCR		
Mp MnSOD-RT-F	CGCATTTCAACCCTTACCTGT	qRT-PCR forward primer
Mp MnSOD-RT-R	ATAGCCCGTCCAACAACACT	qRT-PCR reversed primer
Primers for ORF amplification		
Mp MnSOD-ORF-F	GCGGATCCATGTTAACGGTGCTAG CGCTGTGCG	ORF forward primer
Mp MnSOD-ORF-R	CCGCTCGAGCGGTTACGTAAGCGA TAACGCCACAAG	ORF reversed primer